Cell Reports, Volume *35*

Supplemental information

p53-intact cancers escape tumor suppression through loss of long noncoding RNA *Dino*

Christina B. Marney, Erik S. Anderson, Mutayyaba Adnan, Kai-Lin Peng, Ya Hu, Nils Weinhold, and Adam M. Schmitt

Supplemental Information

This PDF file includes:

Supplemental References
Figures S1- S5
Tables S1 to S4

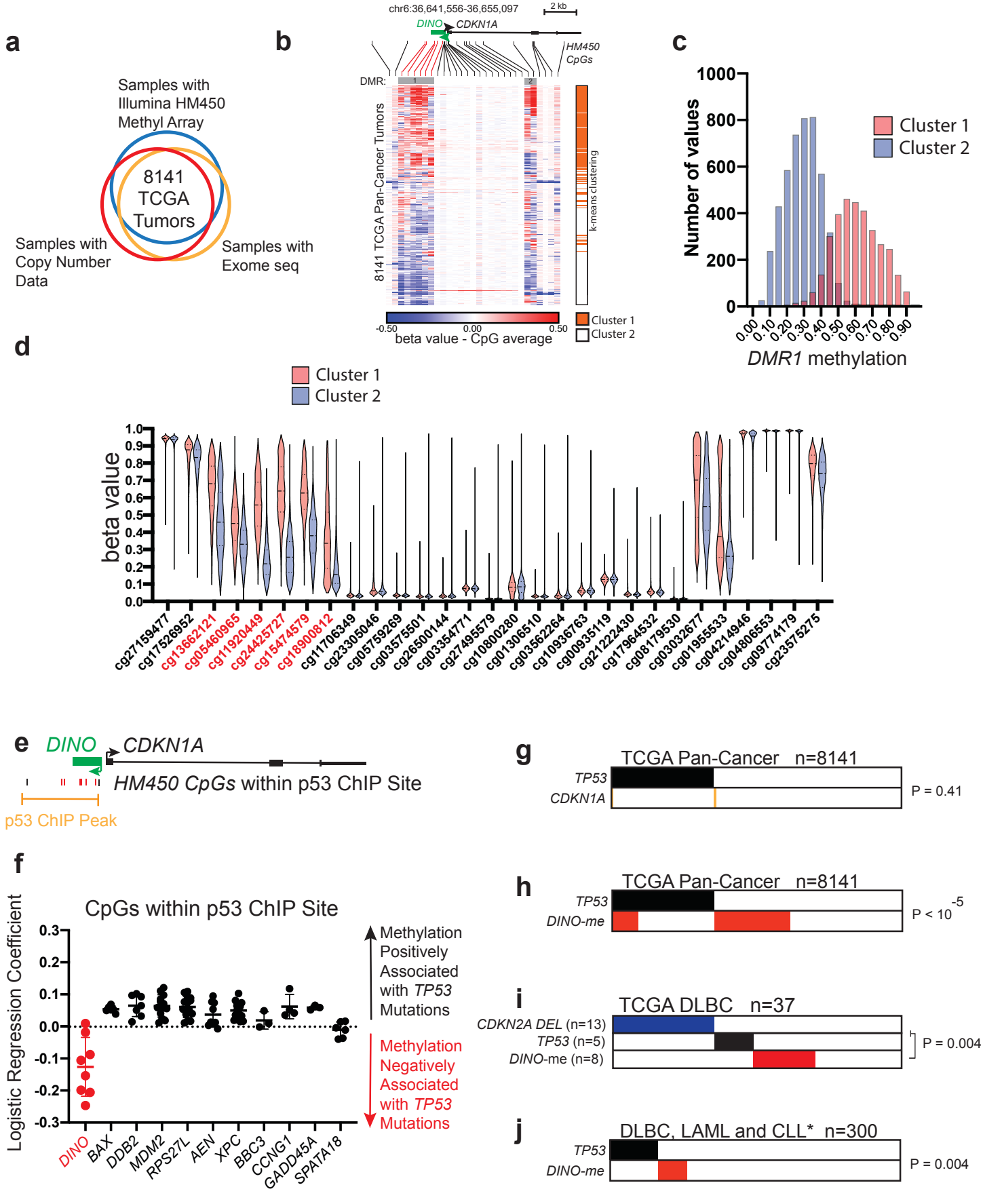
a
Samples with Illumina HM450 Methyl Array
8141 TCGA Tumors
Samples with Copy Number Data
Samples with Exome seq
b
chr6:36,641,556-36,655,097
2 kb
DINO
CDKN1A
HM450 CpGs
DMR:
8141 TCGA Pan-Cancer Tumors
k-means clustering
-0.50
0.00
0.50
beta value - CpG average
Cluster 1
Cluster 2
c
Number of values
1000
800
600
400
200
0
Cluster 1
Cluster 2
0.00 0.10 0.20 0.30 0.40 0.50 0.60 0.70 0.80 0.90
DMR1 methylation
d
Cluster 1
Cluster 2
beta value
1.0 0.9 0.8 0.7 0.6 0.5 0.4 0.3 0.2 0.1 0.0
cg27159477 cg17526952 cg13662121 cg05460965 cg11920449 cg24425727 cg15474579 cg18900812 cg11706349 cg23305046 cg05759269 cg03575501 cg26500144 cg03354771 cg27495579 cg10800280 cg01306510 cg03562264 cg10936763 cg00935119 cg21222430 cg17964532 cg08179530 cg03032677 cg01955533 cg04214946 cg04806553 cg09774179 cg23575275
e
DINO
CDKN1A
HM450 CpGs within p53 ChIP Site
p53 ChIP Peak
f
CpGs within p53 ChIP Site
Logistic Regression Coefficient
0.3 0.2 0.1 0.0 -0.1 -0.2 -0.3
DINO BAX DDB2 MDM2 RPS27L AEN XPC BBC3 CCNG1 GADD45A SPATA18
Methylation Positively Associated with TP53 Mutations
Methylation Negatively Associated with TP53 Mutations
g
TCGA Pan-Cancer n=8141
TP53
CDKN1A
P = 0.41
h
TCGA Pan-Cancer n=8141
TP53
DINO-me
P < 10-5
i
TCGA DLBC n=37
CDKN2A DEL (n=13)
TP53 (n=5)
DINO-me (n=8)
P = 0.004
j
DLBC, LAML and CLL* n=300
TP53
DINO-me
P = 0.004

Figure S1. Identification of differentially methylated regions at the *DINO/CDKN1A* locus. Related to Figure 1. a, Selection criteria for TCGA Pan-Cancer samples in this study. **b**, Relative methylation at HM450 CpGs covering the *DINO/CDKN1A* locus in TCGA Pan-Cancer samples. Above: red lines indicate the position of differentially methylated CpGs downstream of the *DINO* TSS. In this scale, 0 represents average beta value at each CpG across all Pan-Cancer samples. **c**, Histogram of average *DINO* methylation in methylated (Cluster 1) and unmethylated (Cluster 2) clusters in the Pan-Cancer dataset. Average methylation of 0.5 provides the optimal cutoff to distinguish the two clusters. **d**, Violin plots for methylation values at each HM450 CpG at the *DINO/CDKN1A* locus methylated and unmethylated clusters of TCGA Pan-Cancer samples, mean +/- standard deviation. **e**, Location of 8 Illumina HM450 CpGs within the human p53 ChIP peak at the *DINO/CDKN1A* locus previously described (Younger et al., 2015). **f**, Coefficient for logistic regression analyses for the association between methylation values at individual HM450 CpGs within define p53 ChIP peaks at p53-regulated genes that are most strongly associated with *TP53* status in the Pan-Cancer dataset, mean +/- standard deviation (Knijnenburg et al., 2018). **g**, Alteration matrix for *TP53* and *CDKN1A* in the TGCA Pan-Cancer samples. **h**, Alteration matrix for *TP53* and methylated *DINO* in the TGCA Pan-Cancer samples. **i**, Alteration matrix for *TP53*, *CDKN2A* and methylated *DINO* in TCGA DLBC samples. In the TCGA DLBC dataset, methylated *DINO* and *TP53* alterations trended towards mutual exclusivity, but this did not reach statistical significance due to the small number of DLBC samples with copy number, somatic mutation, and methylation data (n = 37). However, deep deletions of *CDKN2A*, encoding the upstream activator of the p53 tumor suppressor pathway p14ARF, are far more prevalent than *TP53* alterations in DLBC. Methylated *DINO* is mutually exclusive with *CDKN2A* deep deletions individually (P = 0.015) and *CDKN2A* and *TP53* alterations (P = 0.004). **j**, Alteration matrix for methylated *DINO* and *TP53* in a combined dataset of three hematologic malignancies including TCGA DLBC, TCGA LAML, and a chronic lymphocytic leukemia samples (Yosifov et al., 2020) demonstrates that methylated *DINO* and *TP53* are mutually exclusive in hematologic malignancies.

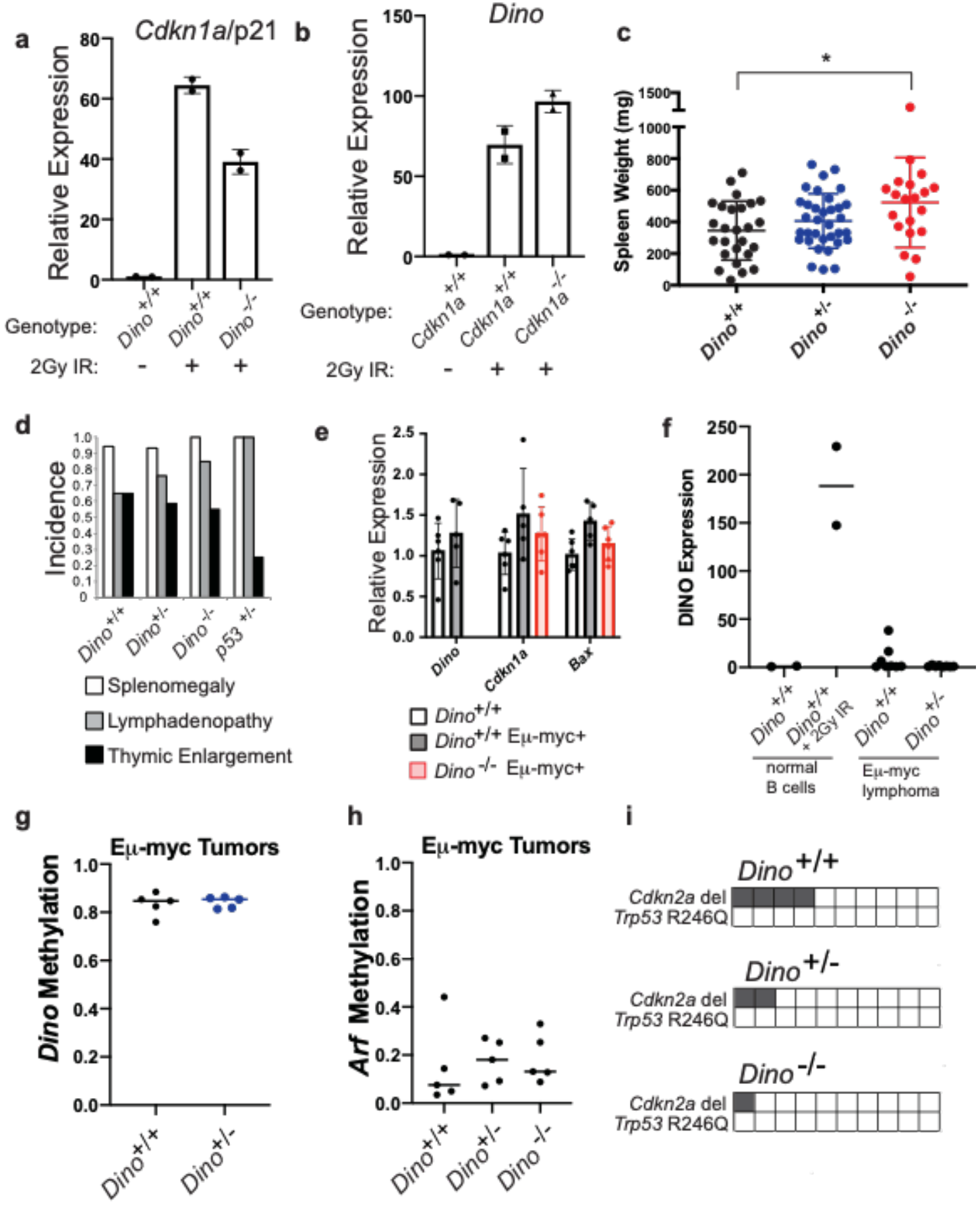
a
Cdkn1a/p21
Relative Expression
Genotype:
2Gy IR:
b
Dino
Relative Expression
Genotype:
2Gy IR:
c
Spleen Weight (mg)
d
Incidence
Splenomegaly
Lymphadenopathy
Thymic Enlargement
e
Relative Expression
Dino
Cdkn1a
Bax
Eμ-myc+
f
DINO Expression
2Gy IR
normal B cells
Eμ-myc lymphoma
g
Eμ-myc Tumors
Dino Methylation
h
Eμ-myc Tumors
Arf Methylation
i
Cdkn2a del
Trp53 R246Q

Figure S2. Dino is required for tumor suppression of mouse Eμ-myc B cell lymphoma. Related to Figure 1. a, Expression of *Cdkn1a* in B cells of indicated *Dino* genotype 6 hours after 2Gy irradiation, mean +/- standard deviation. **b**, Expression of *Dino* in B cells of indicated *Cdkn1a* genotype 6 hours after 2Gy irradiation, mean +/- standard deviation. **c**, Spleen weight at time of death in Eμ-myc mice of indicated genotypes (mean +/- standard deviation, *P=0.01, two-tailed T-test). **d**, Incidence of organ involvement by Eμ-myc lymphoma in mice of indicated genotype. **e**, Expression of indicated genes in splenic B cells isolated from postnatal day 32 mice of indicated *Dino* and Eμ-myc genotypes, mean +/- standard deviation. **f**, Dino expression in normal B cells following sham irradiation or 2Gy irradiation in comparison to Dino expression in Eμ-myc lymphomas from $Dino^{+/+}$ and $Dino^{+/-}$ mice. **g-h**, average CpG methylation in lymphoma samples from Eμ-myc+ mice of indicated *Dino* genotype at the *Dino* locus (**g**) and C*dkn2a/Arf* locus (**h**). **i**, alteration matrix for *Cdkn2a/Arf* deletion or *Trp53 R246Q* mutations in lymphomas from Eμ-myc+ mice of indicated *Dino* genotype.

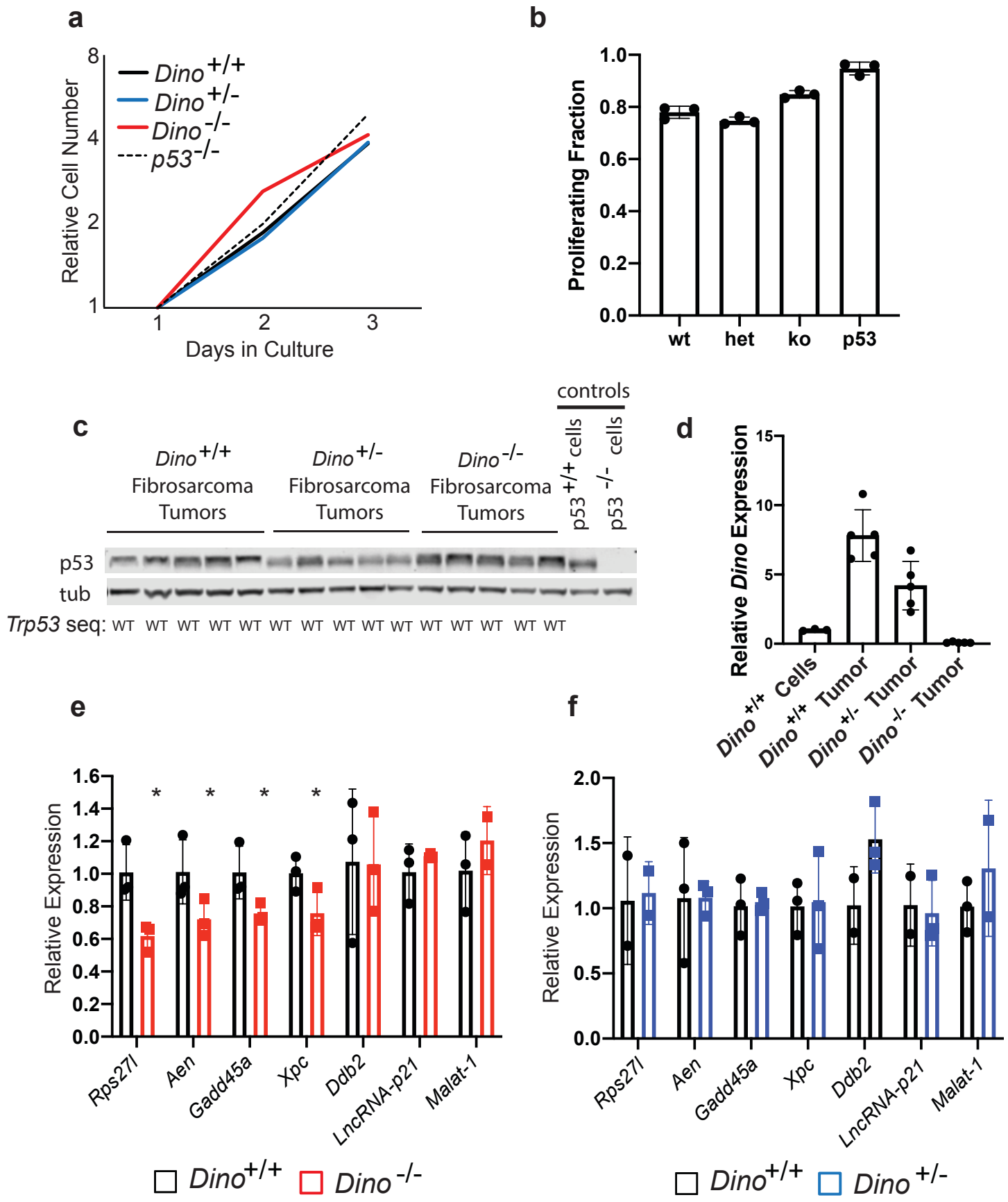
a
Relative Cell Number
Days in Culture
Dino +/+
Dino +/-
Dino -/-
p53 -/-
b
Proliferating Fraction
wt
het
ko
p53
c
Dino +/+ Fibrosarcoma Tumors
Dino +/- Fibrosarcoma Tumors
Dino -/- Fibrosarcoma Tumors
controls
p53 +/+ cells
p53 -/- cells
p53
tub
Trp53 seq: WT WT WT WT WT WT WT WT WT WT WT WT WT WT WT
d
Relative Dino Expression
Dino +/+ Cells
Dino +/+ Tumor
Dino +/- Tumor
Dino -/- Tumor
e
Relative Expression
Rps27l
Aen
Gadd45a
Xpc
Ddb2
LncRNA-p21
Malat-1
Dino+/+
Dino -/-
f
Relative Expression
Rps27l
Aen
Gadd45a
Xpc
Ddb2
LncRNA-p21
Malat-1
Dino+/+
Dino +/-

Figure S3. *Dino* suppresses mouse fibrosarcoma. Related to Figure 2. **a**, *in vitro* proliferation assay in E1A, H-ras^{G12V} MEFs of indicated genotype. **b**, Percentage of E1A, H-ras^{G12V} MEFs of indicated genotype that are EdU+ during tissue culture. **c**, western blot of p53 and β-tubulin in fibrosarcoma tumors of indicated genotype at the endpoint of in vivo tumor formation, in vitro *p53*$^{+/+}$ and *p53*$^{-/-}$ E1A, H-ras^{G12V} MEFs used as a positive and negative control for p53 western. *Trp53* sequencing of these samples revealed all tumors remained *Trp53* wildtype. **d**, *Dino* expression in E1A, H-ras^{G12V} MEFs prior to engraftment (cells) and in fibrosarcoma tumors at the endpoint of *in vivo* tumor formation. **e-f**, The expression of p53-induced genes in *Dino*$^{-/-}$ E1A-Hras^{G12V} cells (**e**) and *Dino*$^{+/-}$ E1A-Hras^{G12V} cells (f) relative to *Dino*$^{+/+}$ E1A-Hras^{G12V} controls. (**e**, mean +/- standard deviation, *Rps27l*, P=0.01*, Aen*, P=0.05, *Gadd45a*, P=0.03, *Xpc*, P=0.03, two-tailed T-test), (**f**, mean +/- standard deviation).

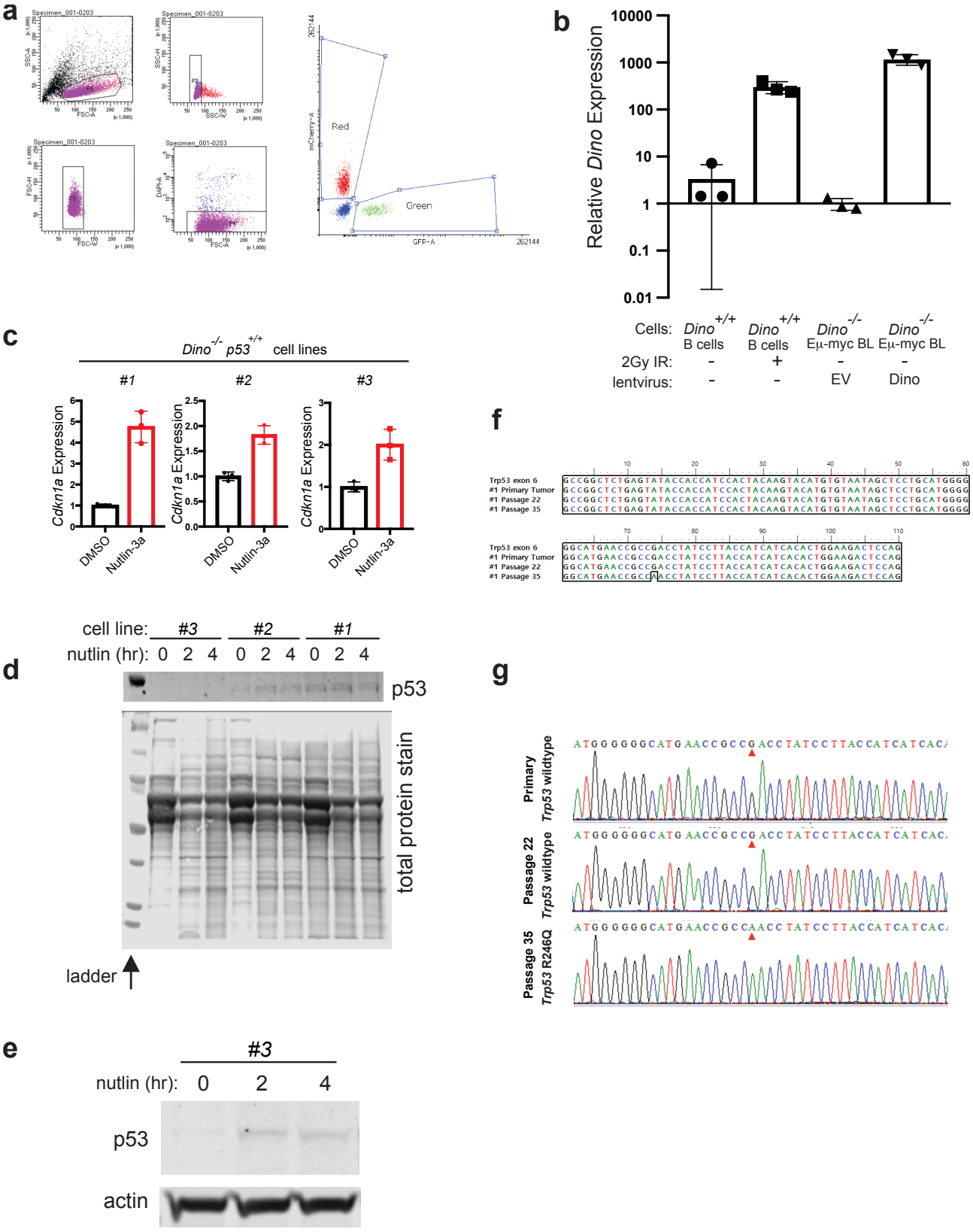
a
Specimen_001-0203
SSC-A
FSC-A
SSC-H
SSC-W
FSC-H
FSC-W
DAPI-A
mCherry-A
GFP-A
Red
Green
b
Relative Dino Expression
10000
1000
100
10
1
0.1
0.01
Cells: Dino+/+ B cells
Dino+/+ B cells
Dino-/- Eμ-myc BL
Dino-/- Eμ-myc BL
2Gy IR: - + - -
lentivirus: - - EV Dino
c
Dino-/- p53+/+ cell lines
#1
#2
#3
Cdkn1a Expression
DMSO
Nutlin-3a
d
cell line: #3 #2 #1
nutlin (hr): 0 2 4 0 2 4 0 2 4
p53
total protein stain
ladder
e
#3
nutlin (hr): 0 2 4
p53
actin
f
Trp53 exon 6
#1 Primary Tumor
#1 Passage 22
#1 Passage 35
g
Primary Trp53 wildtype
Passage 22 Trp53 wildtype
Passage 35 Trp53 R246Q

Figure S4. Development of Eμ-myc lymphoma growth competition assay. Related to Figures 3-4. a, Representative flow cytometry and gates for B lymphoma cells infected with GFP or mCherry expressing lentivirus. **b**, Expression of Dino in *Dino*$^{+/+}$ B cells either 6hr after 2Gy radiation or in *Dino*$^{-/-}$ B lymphoma cells after infection with EV-GFP or Dino-GFP lentivirus, mean +/- standard deviation. All animals used in this experiment were *p53*$^{+/+}$. **c**, Nutlin-3a induced, p53-dependent *CDKN1A* expression in three *Dino*$^{-/-}$ Eμ-myc lymphomas that were adapted to cell culture and retained wild-type *p53* as confirmed by sequencing, (mean +/- standard deviation, #1 P=0.001, #2 P=0.002, #3 P=0.01, two-tailed T-test). **d**, western blot for p53 after 2-4 hours of nutlin treatment in three *Dino*$^{-/-}$ Eμ-myc lymphoma cell lines. Total protein was used as a loading control since standard house keeping genes β-tubulin and actin showed significant variability between cell lines. **e**, western blot for cell line 3 after loading a larger amount of protein lysate confirms p53 protein expression after nutlin treatment in this cell line. **f**, *Trp53* exon 6 sequence in *Dino*$^{-/-}$ B lymphoma cell line #1 at early and late passages. **g**, Chromatograph for *Trp53* exon 6 sequences of samples in C in region of *p53*^{R246Q} mutation.

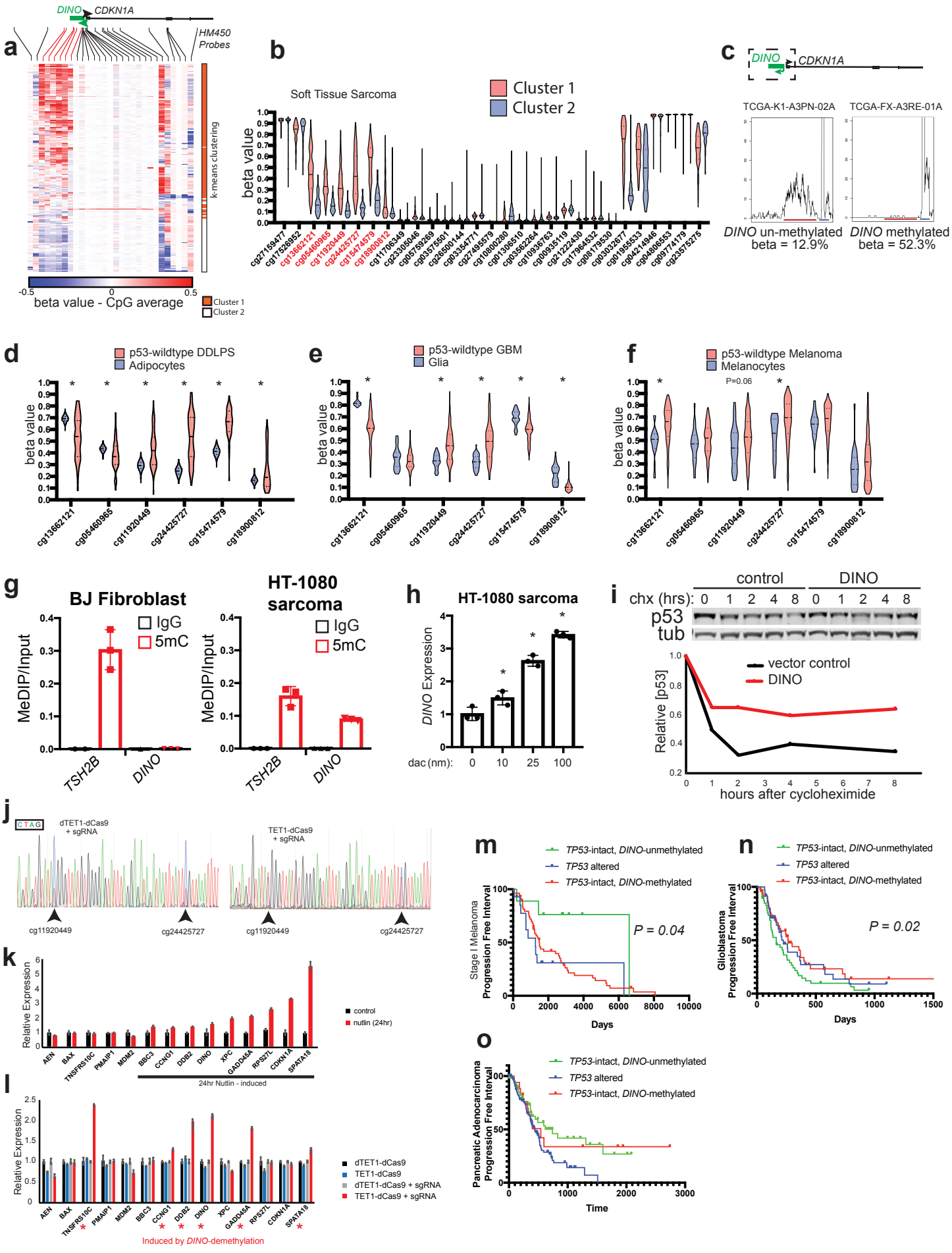
a
DINO
CDKN1A
HM450 Probes
k-means clustering
-0.5
0
0.5
beta value - CpG average
Cluster 1
Cluster 2
b
Soft Tissue Sarcoma
Cluster 1
Cluster 2
beta value
cg27159477
cg17526952
cg13662121
cg05460965
cg11920449
cg24425727
cg15474579
cg18900812
c
DINO
CDKN1A
TCGA-K1-A3PN-02A
TCGA-FX-A3RE-01A
DINO un-methylated
beta = 12.9%
DINO methylated
beta = 52.3%
d
p53-wildtype DDLPS
Adipocytes
beta value
e
p53-wildtype GBM
Glia
f
p53-wildtype Melanoma
Melanocytes
P=0.06
g
BJ Fibroblast
HT-1080 sarcoma
IgG
5mC
MeDIP/Input
TSH2B
DINO
h
HT-1080 sarcoma
DINO Expression
dac (nm):
0
10
25
100
i
control
DINO
chx (hrs):
0 1 2 4 8 0 1 2 4 8
p53
tub
vector control
DINO
Relative [p53]
hours after cycloheximide
j
CTAG
dTET1-dCas9 + sgRNA
TET1-dCas9 + sgRNA
cg11920449
cg24425727
cg11920449
cg24425727
k
Relative Expression
control
nutlin (24hr)
AEN
BAX
TNFRSF10C
PMAIP1
MDM2
BBC3
CCNG1
DDB2
DINO
XPC
GADD45A
RPS27L
CDKN1A
SPATA18
24hr Nutlin - induced
l
Relative Expression
dTET1-dCas9
TET1-dCas9
dTET1-dCas9 + sgRNA
TET1-dCas9 + sgRNA
Induced by DINO-demethylation
m
TP53-intact, DINO-unmethylated
TP53 altered
TP53-intact, DINO-methylated
Stage I Melanoma
Progression Free Interval
P = 0.04
Days
n
TP53-intact, DINO-unmethylated
TP53 altered
TP53-intact, DINO-methylated
Glioblastoma
Progression Free Interval
P = 0.02
Days
o
TP53-intact, DINO-unmethylated
TP53 altered
TP53-intact, DINO-methylated
Pancreatic Adenocarcinoma
Progression Free Interval
Time

Figure S5. Regulation of *DINO* by methylation in human cancers. Related to Figure 5. a, Methylation at HM450 CpGs covering the *DINO/CDKN1A* locus in TCGA SARC samples. Above: red lines indicate position of differentially methylated CpGs downstream of the *DINO* TSS. In this scale, 0 represents average beta value at each CpG across all SARC samples. **b**, Violin plots of methylation beta values at each HM450 CpG at the *DINO/CDKN1A* locus methylated and unmethylated clusters of TCGA SARC. **c**, Genome browser view of RNAseq for *DINO* expression in SARC samples with indicated *DINO* methylation status. Red line indicates the coordinates of *DINO*; blue line indicates exon 1 of *CDKN1A.* **d**, Violin plot of methylation at each *DINO* CpG in p53-intact dedifferentiated liposarcoma samples and normal adipose tissue, mean +/- standard deviation, * $P<10^{-4}$, two tailed T test. **e**, Violin plot of methylation at each *DINO* CpG in p53-intact glioblastoma samples and normal glia, mean +/- standard deviation, * $P<10^{-4}$, two tailed T test. **f**, Violin plot of methylation at each *DINO* CpG in p53-intact melanoma samples and normal melanocytes, mean +/- standard deviation, * $P<10^{-3}$, two tailed T test. **g**, *DINO* and *TSH2B* methylation in BJ fibroblasts and HT-1080 sarcoma cells as measured by MeDIP, mean +/- standard deviation. **h**, *DINO* expression in HT-1080 cells after treatment with indicated dose of 5-aza-2'-deoxycitidine (dac) for 72 hours (mean +/- standard deviation, 10nm dac P=0.046, 25nM dac P=0.0004, 100nM dac $P=5x10^{-5}$, two-tailed T-test). **i**, quantitative p53 western blot after cycloheximide (chx) chase in HT-1080 cells transfected with pcDNA vector control or pcDNA-DINO. **j**, Sample chromatograms for sequences within the *DINO* DMR after bisulfite conversion of DNA from HT-1080 cells infected with lentivirus expressing sgRNA and TET1-dCas9 or dTET1-dCas9. **k-l**, expression of canonical p53-regulated genes in HT-1080 cells after (**k**) 24 hours of Nutlin-3a treatment or (**l**) in cells infected with indicated CRISPR methylation editing viral constructs (TET1-dCas9 or dTET1-dCas9 with or without a sgRNA targeting the *DINO* DMR). mean+/- standard deviation. **m**, Progression Free Interval in TCGA stage I melanoma patients with tumors of indicated *TP53* and *DINO* methylation status, log-rank test. **n**, Progression Free Interval in glioblastoma patients with tumors of indicated *TP53* and *DINO* methylation status, log-rank test. **o,** Progression Free Interval in pancreatic adenocarcinoma patients with tumors of indicated *TP53* and *DINO* methylation status, log-rank test nonsignificant but patients with *DINO* methylated tumors, like those with *TP53* mutated tumors, had reduced median survival.

	Sample Number	DINOme≥0.5, TP53-wt	DINOme≥0.5, TP53-mut	DINOme<0.5, TP53-wt	DINOme<0.5, TP53-mut	Fisher Exact P
TCGA Pan-Cancer	8141	2145	751	3123	2122	<0.00001
TCGA SKCM	465	318	38	76	33	<0.00001
TCGA GBM	130	48	4	48	30	0.0001
TCGA SARC	229	44	12	88	85	0.0003
TCGA STAD	389	61	27	142	159	0.0003
TCGA PAAD	174	19	10	53	92	0.0065
TCGA LUSC	351	10	16	60	265	0.0209

Table S1. Relationship of *DINO* methylation and *TP53* alterations in select human cancers. Related to Figure 1.

Methylation Cutoff	DINOme≥cutoff, TP53-wt	DINOme≥cutoff, TP53-mut	DINOme<cutoff, TP53-wt	DINOme<cutoff, TP53-mut	Fisher Exact P	TP53 Alt (%), DINOme≥cutoff	TP53 Alt (%), DINOme<cutoff
0.8	77	13	5191	2860	0	0.144444444	0.355235374
0.7	424	130	4844	2743	<0.00001	0.23465704	0.361539475
0.6	1118	370	4150	2503	<0.00001	0.248655914	0.376221254
0.5	2145	751	3123	2122	<0.00001	0.259323204	0.404575786
0.4	3283	1355	1985	1518	<0.00001	0.29215179	0.433342849
0.3	4307	2174	961	699	<0.00001	0.335442061	0.421084337
0.2	4944	2675	324	198	0.2	0.351095944	0.379310345

Table S2. Mutual exclusivity of *TP53* alterations and *DINO* methylation in the Pan-Cancer dataset across multiple methylation cutoff values. Related to Figure 1.

	Chromosome	Start	Stop
CDKN1A	chr6	36643696	36646241
BAX	chr19	49458109	49459140
DDB2	chr11	47236249	47237682
MDM2	chr12	69202420	69203119
RPS27l	chr15	63448812	63450014
AEN	chr15	89164217	89165584
XPC	chr3	14219749	14220446
TNFRSF10C	chr8	22925361	22926664
BBC3	chr19	47734508	47735453
CCNG1	chr5	162864504	162865267
GADD45A	chr1	68152194	68152661
SPATA18	chr4	52917597	52918603

Table S3. Genomic coordinates (Hg19) for p53 ChIP peaks at canonical p53 responsive genes, related to Fig S2A-S2B, from (Younger et al., 2015). Related to Figure 1.

Primer	Species	Sequence	Purpose
Dino F	mouse	tggagacctgatgataccca	Genotyping Dino GFP
Dino R	mouse	aagtctgggactactcagtc	Genotyping Dino GFP
Dino-eGFP R	mouse	gaacttgtggccgtttacgt	Genotyping Dino GFP
IgH-Fwd	mouse	CCTTTCTGTACGGTTGTTCGGG	Genotyping E-mu Myc
Myc Rev	mouse	CCTTTCTGTACGGTTGTTCGGG	Genotyping E-mu Myc
mDino Genomic Locus Fwd	mouse	ggagacctgatgatacccaact	Dino Copy Number Genomic QPCR
mDino Genomic Locus Rev	mouse	gcacacacacacagatgcac	Dino Copy Number Genomic QPCR
Dino-eGFP Fwd	mouse	AAGCTGACCCTGAAGTTCATCTGC	Dino Copy Number Genomic QPCR
Dino-eGFP Rev	mouse	CTTGTAGTTGCCGTCGTCCTTGAA	Dino Copy Number Genomic QPCR
L32 genomic locus Fwd	mouse	TTCCTGGTCCACAATGTCAAG	Dino Copy Number Genomic QPCR - control
L32 genomic locus Rev	mouse	gtctcaggcttcaaccaagg	Dino Copy Number Genomic QPCR - control
DINO-F	human	GGAGGCAAAAGTCCTGTGTT	DINO Genomic qPCR meDIP
DINO-R	human	GGGCTCAGAGAAGTCTGGTG	DINO Genomic qPCR meDIP
TSH2B-F	human	CAGACATCTCCTCGCATCAA	TSH2B Genomic qPCR meDIP
TSH2B-R	human	GGAGGATGAAAGATGCGGTA	TSH2B Genomic qPCR meDIP
mDino-BamHI Fwd	mouse	tatataGGATCCgtagaaTTCAGTGCAGGGTGGTGGAGA	mDino cloning into lentiviral vector
mDino-NotI Rev	mouse	tatataGCGGCCGCgtaAGTTTGAACGGATATCTTTAGTTAAAAGATCA	mDino cloning into lentiviral vector
pCDHvirusEF1a-Forward	plasmid	TCAAGCCTCAGACAGTGGTTC	pCDH-EF1α-MCS-(PGK-GFP-T2A-Puro) sequencing
DINO_DMR-1F	human	AGAGAGTTTYGGGTAGGAGGTAAAAGTTTTGTG	bisulfite sequencing
DINO_DMR-1R	human	CTCCCTACACCCTACACTCACCTAAAC	bisulfite sequencing
DINO_DMR-2F	human	TGGAGATTAGGTTGTTTTTTTTTGGTAG	bisulfite sequencing
DINO_DMR-2R	human	AAACAAAAATTTACCCAATACAACTAAAAAAATC	bisulfite sequencing
TSH2B_DMR_F	human	TGTTATTTGATTGGTTGATGGT	bisulfite sequencing
TSH2B_DMR_R	human	CTTTCTTAAAACCCTTCTTA	bisulfite sequencing
Dino_me1_F	mouse	AATGTTATTTTTATTTGAGAAGTTTGGA	bisulfite sequencing
Dino_me1_R	mouse	ATCCTATTCAAAAACACAATTAAAAAAC	bisulfite sequencing
Dino_me2_F	mouse	GTTTTTTAATTGTGTTTTTGAATAGGAT	bisulfite sequencing
Dino_me2_R	mouse	AAACTATAAATTCTAACATCTACTCTCC	bisulfite sequencing
Cdkn2a_me_F	mouse	GGGTTTTTTTTATTTGGTTTAGGATT	bisulfite sequencing
Cdkn2a_me_R	mouse	CRCAAATTCTTAATCACTATAAAAATTC	bisulfite sequencing
mDino QPCR Fwd	mouse	gcaatggtgtgcctgactat	RT-qPCR
mDino QPCR Rev	mouse	acttctggcttcccagagc	RT-qPCR
hDINO QPCR Fwd	human	gggctcagagaagtctggtg	RT-qPCR
hDINO QPCR Rev	human	ggaggcaaaagtcctgtgtt	RT-qPCR
mBax QPCR Fwd	mouse	TGAAGACAGGGGCCTTTTTG	RT-qPCR
mBax QPCR Rev	mouse	AATTCGCCGGAGACACTCG	RT-qPCR
hBAX_fwd	human	TCTGACGGCAACTTCAACTG	RT-qPCR
hBAX_rev	human	CAGCCCATGATGGTTCTGAT	RT-qPCR
mCdkn1a Fwd	mouse	cacagctcagtggactggaa	RT-qPCR
mCdkn1a Rev	mouse	accctagacccacaatgcag	RT-qPCR
hCDKN1A Fwd	human	gaggccgggatgagttgggaggag	RT-qPCR
hCDKN1A rev	human	cagccggcgtttggagtggtagaa	RT-qPCR
mB-actin Fwd	mouse	tcctagcaccatgaagatcaagatc	RT-qPCR
mB-actin Rev	mouse	ctgcttgctgatccacatctg	RT-qPCR
hB-ACTIN Fwd	human	catgtacgttgctatccaggc	RT-qPCR
hB-ACTIN Rev	human	ctccttaatgtcacgcacgat	RT-qPCR
hGAPDH Fwd	human	gagtcaacggatttggtcgt	RT-qPCR
hGAPDH Rev	human	ttgattttggagggatctcg	RT-qPCR
mAen_Fwd	mouse	CACAAGGCTATCCCCTTTCA	RT-qPCR
mAen_Rev	mouse	GAGGGTGGACGTACTTCAGG	RT-qPCR
hAEN_Fwd	human	CATCACTCGGCAGCACAT	RT-qPCR
hAEN_Rev	human	ACTTGAGCGCCTGGAAGTC	RT-qPCR
mRps27l_Fwd	mouse	CTATCCCGGAAGTTGCTGAG	RT-qPCR
mRps27l_Rev	mouse	TCCAAGGAAGGGTGTAACAGA	RT-qPCR
hRPS27L_Fwd	human	ATCCGTCCTTGGAAGAGGAA	RT-qPCR
hRPS27L_Rev	human	GCTGAAAACCGTGGTGATCT	RT-qPCR
mXpc_Fwd	mouse	CCGAGGACAACAAAGTAGCC	RT-qPCR
mXpc_Rev	mouse	CCCCTCTTCCTCTTTCCTTG	RT-qPCR
hXPC_Fwd	human	AAAGAAAGTGGCCAAGGTGA	RT-qPCR
hXPC_Rev	human	CAGATGGTGTGCCTTCTTGA	RT-qPCR
mDdb2_Fwd	mouse	AAATGCCCAGAAACCCAGAAG	RT-qPCR
mDdb2_Rev	mouse	GTCCTGCTAGAAACGGGACC	RT-qPCR

hDDB2_Fwd	human	TATTACGCCCCAGGAACAAG	RT-qPCR
hDDB2_Rev	human	TATTCAAGCAGCAGGCACAG	RT-qPCR
mGadd45a_fwd	mouse	CCGAAAGGATGGACACGGTG	RT-qPCR
mGadd45a_Rev	mouse	TTATCGGGGTCTACGTTGAGC	RT-qPCR
hGADD45a_Fwd	human	ATGGATCAATGGGTTCCAGT	RT-qPCR
hGADD45a_Rev	human	CCTTGCATCAGTGTAGGGAGT	RT-qPCR
mBbc3_Fwd	mouse	GCG GCG GAG ACA AGA AGA	RT-qPCR
mBbc3_Rev	mouse	AGT CCC ATG AAG AGA TTG TAC ATG AC	RT-qPCR
hBBC3_fwd	human	GATGGACTCAGCATCGGAAG	RT-qPCR
hBBC3_rev	human	CACCAGCACAACAGCCTTT	RT-qPCR
mCcng1_Fwd	mouse	CGTGTCC TCAGTTCTTTGGC TTTGACACG	RT-qPCR
mCcng1_Rev	mouse	GATGCTTCGCCTGTACCTTCATT	RT-qPCR
hCCNG1_Fwd	human	CCTTCTGTGTTGGCATTGTCTATC	RT-qPCR
hCCNG1_Rev	human	CAAGCTCTTGCCAGAAGGTCAG	RT-qPCR
mPerp_Fwd	mouse	GACCCCAGATGCTTGTTTTC	RT-qPCR
mPerp_Rev	mouse	CAGCAGGGTTATCGTGAAGC	RT-qPCR
mMdm2_Fwd	mouse	GGACTCGGAAGATTACAGCCTGA	RT-qPCR
mMdm2_Rev	mouse	TGTCTGATAGACTGTGACCCG	RT-qPCR
hMDM2_fwd	human	GAAGGAAACTGGGGAGTCTTG	RT-qPCR
hMDM2_rev	human	GGTGGTTACAGCACCATCAG	RT-qPCR
mPmaip1_Fwd	mouse	GCAGAGCTACCACCTGAGTTC	RT-qPCR
mPmaip1_Rev	mouse	CTTTTGCGACTTCCCAGGCA	RT-qPCR
hPMAIP1_fwd	human	AGCTGGAAGTCGAGTGTGCT	RT-qPCR
hPMAIP1_rev	human	TTTTTGATGCAGTCAGGTTCC	RT-qPCR
hTNFRSF10C_F	human	GGTGTGGATTACACCAACGCTTC	RT-qPCR
hTNFRSF10C_R	human	CTGACACACTGTGTCTCTGGTC	RT-qPCR
mMalat1_Fwd	mouse	ggcggaattgctggtagttt	RT-qPCR
mMalat1_Rev	mouse	agcatagcagtacacgcctt	RT-qPCR
mlncp21_Fed	mouse	GGAGTCTCATGCTCAGAGAAGAA	RT-qPCR
mlncp21_Rev	mouse	CCCTGACAGACAAGTACCCTCT	RT-qPCR
mmTrp53exon1F	mouse	TGGATGTCCCACCTTCTTTT	gDNA sequencing
mmTrp53exon1R	mouse	GATACAGGTATGGCGGGATG	gDNA sequencing
mmTrp53exon2-3F	mouse	GGACTGCAGGGTCTCAGAAG	gDNA sequencing
mmTrp53exon2-3R	mouse	CTGAAGAGGAACCCCCAAAT	gDNA sequencing
mmTrp53ex4-5F	mouse	TGGTGCTTGGACAATGTGTT	gDNA sequencing
mmTrp53ex4-5R	mouse	TAGCACTCAGGAGGGTGAGG	gDNA sequencing
mmTrp53ex6F	mouse	CCCTACTCTACAACTAAAACTGAAACT	gDNA sequencing
mmTrp53ex6R	mouse	GGGACTCGTGGAACAGAAAC	gDNA sequencing
mmTrp53ex7-8F	mouse	GGGGGCCTAGTTTACACACA	gDNA sequencing
mmTrp53ex7-8R	mouse	ATGCGAGAGACAGAGGCAAT	gDNA sequencing
mmTrp53ex9F	mouse	CAAAACAAAAACCTGTAAGTGGA	gDNA sequencing
mmTrp53ex9R	mouse	GGTGCAGCCCTAAGCATCTA	gDNA sequencing
mmTrP53ex10F	mouse	GATGATGGTGGTGGTGATGA	gDNA sequencing
mmTrP53ex10R	mouse	CTACTCAGAGAGGGGGCTGA	gDNA sequencing

Name	Source	ID	Reference
pCDH-EF1α-MCS-(PGK-GFP-T2A-Puro)	System Biosciences	CD813A-1	
pBabe 12S E1A	Addgene	18742	*(Samuelson and Lowe, 1997)*
pWZL hygro H-Ras V12	Addgene	18749	*(Serrano et al., 1997)*
pBABE-zeo	Addgene	1766	*(Morgenstern and Land, 1990)*
Fuw-dCas9-Tet1CD-P2A-BFP,	Addgene	108245	*(Liu et al., 2018)*
Fuw-dCas9-dead Tet1CD-P2A-BFP	Addgene	108246	*(Liu et al., 2018)*

pgRNA-modified	Addgene	84477	*(Liu et al., 2016)*

Table S4. Primers and plasmids used in the study. Related to Figures 1, 2, 4, and 5.